

A comparison of the dinuclear diacyl complexes $\text{FpC(O)(CX}_2)_3\text{C(O)Fp}$ ($\text{X}=\text{F}$ or H ; $\text{Fp}=\eta^5\text{-C}_5\text{H}_5\text{Fe(CO)}_2$) and the molecular structure of the compound where $\text{X}=\text{F}$

Steve J. Archer, Grant A. Harvey, John R. Moss*

Department of Chemistry, University of Cape Town, Rondebosch 7700 (South Africa)

and Andrew M. Crouch

Department of Chemistry, University of the Western Cape, Bellville 7535 (South Africa)

(Received December 19, 1991; revised May 12, 1992)

Abstract

The dinuclear diacyl compounds $\text{FpC(O)(CX}_2)_3\text{C(O)Fp}$ have been obtained in good yields (66%, $\text{X}=\text{H}$, 57%, $\text{X}=\text{F}$) from the reactions of NaFp with $\text{ClC(O)(CX}_2)_3\text{C(O)Cl}$ (where $\text{Fp}=\eta^5\text{-C}_5\text{H}_5\text{Fe(CO)}_2$). The compounds have been characterized by IR, NMR (^1H , ^{13}C and ^{19}F) and mass spectrometry. The thermal behaviour of both compounds has been examined by differential scanning calorimetry (DSC) and the electrochemical behaviour by cyclic voltammetry (CV). Some reactions have been carried out on both of the complexes and the data are compared and discussed. The molecular structure of $\text{FpC(O)(CF}_2)_3\text{C(O)Fp}$ has been determined by X-ray crystallography and is discussed.

Introduction

Transition metal acyl complexes MC(O)R are key intermediates in stoichiometric and catalytic reactions involving carbon monoxide [1]. Important catalytic reactions involving acyl species include the hydroformylation reaction of alkenes and the synthesis of acetic acid using rhodium catalysts. Mononuclear acyl complexes have thus been well studied. Binuclear acyl complexes may also prove to be important intermediates in catalytic cycles leading to the production of bifunctional organic compounds including diols, diols and diacids, however very little work has been carried out on such complexes. Fluorocarbon compounds are becoming increasingly important and perfluoro organometallic complexes may be important intermediate species in their production.

We now report on a comparative study of two binuclear diacyl complexes, namely $\text{FpC(O)(CH}_2)_3\text{C(O)Fp}$ and its fluorocarbon analogue $\text{FpC(O)(CF}_2)_3\text{C(O)Fp}$, where $\text{Fp}=\eta^5\text{-C}_5\text{H}_5\text{Fe(CO)}_2$.

Experimental

Reactions were carried out under an atmosphere of nitrogen using standard Schlenk techniques. Tetrahy-

drofuran (THF) was distilled from sodium wire. The compound $[(\eta^5\text{-C}_5\text{H}_5)\text{Fe(CO)}_2]_2$ (Fp_2) was purchased from Strem Chemicals, USA and $\text{ClCO(CF}_2)_3\text{COCl}$ from ICN Biomedicals Inc., New York. The compound Fp_2 was converted to NaFp using a well-documented procedure [2]. Alumina used for column chromatography (deactivated, 70–230 mesh) was purchased from Merck. IR spectra were recorded on a Perkin-Elmer 983 spectrophotometer. NMR spectra were recorded on Bruker WH90 or Varian VXR 200 spectrometers. Tetramethylsilane was used as internal standard for ^1H and ^{13}C NMR spectra and trifluoroacetic acid used for ^{19}F NMR. Mass spectra were recorded on a VG Micromass 16F spectrometer operating at 70 eV using a direct probe and source temperature in the range 80–100 °C. Differential scanning calorimetry was carried out on a Du Pont 9900 thermal analyzer. Samples were heated in aluminium pans which had been hermetically sealed in air.

Preparation of $\text{FpC(O)(CF}_2)_3\text{C(O)Fp}$ (1)

Perfluoroglutaryl chloride (0.77 g, 2.77 mmol) was added dropwise with stirring over 5 min to a solution of NaFp (5.65 mmol) in THF (20 ml) at -78 °C. The reaction mixture was stirred at this temperature for a further 10 min, then allowed to warm to room temperature over 20 min and then stirred for a further

*Author to whom correspondence should be addressed.

1 h. The solvent was removed under reduced pressure leaving a brown oily residue. The oil was triturated with water and the resulting brown solid filtered off to give a crude product (1.31 g, 84%). This solid was recrystallized from CH_2Cl_2 /hexane to give fine yellow crystals of $\text{FpC(O)(CF}_2)_3\text{C(O)Fp}$ (0.89 g, 57%), m.p. 113–115 °C. The product was identified by comparison with reported data for this compound [3] and by the following data: IR (CH_2Cl_2) $\nu(\text{CO})$ 2040(vs) 1988(vs) 1647(m) cm^{-1} ; $^1\text{H NMR}$ (CDCl_3) δ 4.95 (singlet) (C_5H_5); $^{19}\text{F NMR}$ (CDCl_3) δ -0.51 (singlet) ($\alpha\text{-CF}_2$), δ -6.13 (singlet) ($\beta\text{-CF}_2$); $^{13}\text{C NMR}$ (CDCl_3) δ 86.4 (singlet) (C_5H_5), δ 105.9 (triplet of triplets) $^1\text{J}(\text{C-F})$ 270 Hz, $^2\text{J}(\text{C-F})$ 31 Hz ($\alpha\text{-CF}_2$), δ 112.5 (triplet of triplets) $^1\text{J}(\text{C-F})$ 267 Hz, $^2\text{J}(\text{C-F})$ 34 Hz ($\beta\text{-CF}_2$), δ 212 (singlet) (terminal Fe-CO); mass spectrometry shows the highest m/e peak at 476 corresponding to $M-3\text{CO}$ and other significant peaks at m/e 308, 289, 261, 205, 186, 177, 149, 121, 91 and 56; DSC shows: T_{max} endo 115, T_{max} exo 237 and 375 °C.

Preparation of $\text{FpC(O)(CH}_2)_3\text{C(O)Fp}$ (**2**)

This was prepared in a similar way from NaFp (5.25 mmol), glutaryl chloride (3.08 mmol) and THF (20 ml). The crude product (1.30 g) was recrystallized from CH_2Cl_2 /hexane to give golden orange platelets of $\text{FpC(O)(CH}_2)_3\text{C(O)Fp}$ (0.85 g, 67%), m.p. 110–112 °C. The product was identified by comparison with reported data [3] and by the following: IR (CH_2Cl_2) $\nu(\text{CO})$ 2017(vs) 1957(vs) 1640(m); $^1\text{H NMR}$ (CDCl_3) δ 1.61 (quintet 2H) $^3\text{J}(\text{H-H})$ 7.1 Hz ($\beta\text{-CH}_2$), δ 2.83 (triplet 4H) $^3\text{J}(\text{H-H})$ 7.1 Hz ($\alpha\text{-CH}_2$), δ 4.83 (singlet, 10H) (C_5H_5); $^{13}\text{C NMR}$ (CDCl_3) δ 21.1 ($\beta\text{-CH}_2$) δ 65.1 ($\alpha\text{-CH}_2$), δ 86.3 (C_5H_5), δ 214.3 terminal (Fe-CO), δ 256.5 [$\text{Fe-CO}(\text{acyl})$]; mass spectrometry shows the highest m/e ion at 368 corresponding to $M-3\text{CO}$ with other main peaks at m/e 340, 326, 312, 298, 274, 269, 243, 217, 205, 187, 177, 149, 120, 91 and 56; DSC shows: T_{max} endo 115, T_{max} exo 210, T_{max} endo 277 and T_{max} exo 400 °C.

Cyclic voltammetry studies

These were carried out in acetonitrile solution using 0.1 M NaClO_4 as background electrolyte in a 25 ml cell. The working and counter electrodes were platinum discs and the reference electrode SCE with a Luggin capillary. Potentials were controlled by an Amel potentiostat and scanned with an Amel function generator. Under these conditions the ferrocene/ferricinium (Fe/Fe^+) couple showed a potential of 0.41 V. Voltammograms were recorded on a JJ X-Y recorder. Before recording voltammograms, all solutions were thoroughly degassed with ultrapure nitrogen for 15 min. All ex-

periments were carried out at room temperature. Scan rates were 100 mV s^{-1} . Acetonitrile was purified by distilling over sodium metal and stored in contact with molecular sieves. A blank run showed an electrochemical window of 3.1 V in the range -1.1 to +2.0 V. Concentrations used were 3.93×10^{-3} M for compound **1** and 2.21×10^{-3} M for **2**.

Reactivity studies

All reactions of $\text{FpC(O)(CX}_2)_3\text{C(O)Fp}$ ($\text{X}=\text{F, H}$) were carried out in Schlenk tubes. Compounds **1** and **2** were each stirred with:

(a) a large excess of HPF_6 in dry methanol for 50 min at 70 °C;

(b) AgPF_6 (1:1 molar ratio) in dry THF for 3 h at room temperature;

(c) I_2 (1:1 molar ratio) in dry benzene for 20 min at room temperature.

Compounds **1** and **2** were also refluxed with PPh_3 (1:2 molar ratio) in dry THF for several days. The progress of the reactions was monitored by IR and $^1\text{H NMR}$.

X-ray analysis

Suitable single crystals of compound **1** were obtained by slow crystallization of the compound from a CH_2Cl_2 /hexane solution at 0 °C. X-ray analysis was carried out on an Enraf-Nonius CAD4 diffractometer, using $\text{Mo K}\alpha$ ($\lambda=0.7107$ Å) radiation. Cell parameters were obtained from a least-squares analysis of the setting angles of 24 reflections in the range $16 < \theta < 17^\circ$. During data collection, the intensities of three reference reflections were monitored every hour and recentring was checked after every 100 measured reflections. Data were corrected for Lorentz and polarization factors and empirical absorption corrections applied [4]. Crystal data and other experimental data are given in Table 1.

Structure solution

The positions of the two Fe atoms were found from a Patterson map in the space group $P2_1/c$. A series of difference Fouriers then revealed the positions of all remaining non-H atoms. Each cyclopentadienyl ring is disordered over two sites via a $2\pi/10$ rotation about the Fe-Cp (median) axis. Refinement of site occupancy factors of ring carbon atoms indicated relative conformational populations of 65/35 for one of the Cp rings and 80/20 for the other. Erratic bond lengths within the rings necessitated the treatment of the rings as rigid pentagons with C-C bond lengths constrained at 1.42 ± 0.02 Å. The Fe, F and O atoms were treated anisotropically. The ellipticity of the thermal parameters for O and F atoms is pronounced. In the final difference

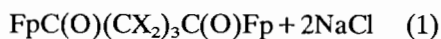
TABLE 1. Crystal data and parameters for data collection and refinement for $\text{FpC(O)(CF}_2)_3\text{C(O)Fp}$ (**1**)

<i>Crystal data</i>	
Molecular formula	$\text{C}_{19}\text{H}_{10}\text{O}_6\text{F}_6\text{Fe}_2$
M_R (g mol^{-1})	559.97
Space group	$P2_1/c$
a (\AA)	7.723(2)
b (\AA)	16.837(3)
c (\AA)	15.767(4)
β ($^\circ$)	94.70(2)
V (\AA^3)	2043.0(6)
D_c for $Z=4$ (g cm^{-3})	2.18
$F(000)$	1312
<i>Data collection</i>	
μ ($\text{Mo K}\alpha$) (cm^{-1})	15.26
Crystal dimensions (mm)	$0.45 \times 0.40 \times 0.30$
Crystal decay (%)	1.3
Scan mode	ω - 2θ
Scan width ($^\circ$)	$(0.85 + 0.35 \tan\theta)$
Aperture width (mm)	$(1.12 + 1.05 \tan\theta)$
θ Range scanned ($^\circ$)	1–25
<i>Refinement</i>	
No. reflections collected	3860
No. reflections observed (with $I_{\text{rel}} > 2\sigma I_{\text{rel}}$)	2533
No. parameters	220
$R = \sum \ F_o\ - F_c / \sum \ F_o\ $	0.0609
$R_w = \sum w^{1/2} \ F_o\ - F_c / \sum w^{1/2} \ F_o\ $	0.0603
Weighting scheme	$5.43(\sigma^2 F)^{-1}$

map, residual electron density was less than 0.5 e \AA^{-3} . Other details of the final refinement are reported in Table 1. The structure was solved using SHELX76 [5]. Complex neutral atom scattering factors were taken from Cromer and Mann [16] and dispersion correction from Cromer and Liberman [7]. PLUTO [8] produced the drawings.

Results and discussion

The diacyl compounds **1** and **2** were prepared by the same route as reported by King [3].



However, our reaction conditions and work-up procedure are significantly different and gave greatly improved yields, particularly for the perfluoro compound. (We found for $X=H$, 67% yield and for $X=F$, 57% yield, compared with 45% and 14%, respectively reported by King [3]).

Characterization data for the dinuclear diacyl complexes

IR data in the $\nu(\text{CO})$ region for **1** and **2** agree well with the literature [3]. We note that the terminal $\nu(\text{CO})$

bands for **2** ($X=H$) are about 25 cm^{-1} lower than for **1** ($X=F$) consistent with weaker terminal C–O bonds and stronger Fe–C(carbonyl) bonds in **2** relative to **1**.

^1H NMR data for **1** and **2** were recorded and assigned (see ‘Experimental’). The ^{13}C NMR spectra for **1** and **2** have not previously been reported. These data are presented and assignments made (see ‘Experimental’). For compound **1** the acyl CO groups were not detected, presumably due to relaxation effects, although they were observed in **2**. The C_α , C_β and cyclopentadienyl carbon atoms of **2** appear at lower chemical shifts than for **1** as may be expected. The ^{19}F NMR spectrum of **1** has also not been reported previously. We observe two broad singlets at $\delta -0.51$ and $\delta -0.12$ which we assign to $\alpha\text{-CF}_2$ and $\beta\text{-CF}_2$, respectively. No F–F couplings were observed, as is also found in $\text{ClC(O)(CF}_2)_3\text{C(O)Cl}$.

Mass spectra of **1** and **2** both show the highest m/e ion corresponding to $M-3\text{CO}$; other main peaks are listed in ‘Experimental’.

To compare the thermal behaviour of **1** and **2**, DSC traces were obtained for the compounds and are given in ‘Experimental’. The first T_{max} (endo) for **1** and **2** is due to melting. The first T_{max} (exo) is probably due to decomposition and it is found that **1** decomposes at a higher temperature than **2**. For **2**, a sharp T_{max} (endo) is seen at $277 \text{ }^\circ\text{C}$ which may be due to some $[\text{CpFe(CO)}_2]_2$ (which shows T_{max} (endo) at $285 \text{ }^\circ\text{C}$). Since this is not seen in **1**, there appear to be different decomposition pathways for **1** and **2**. A high temperature T_{max} (exo) observed for **1** and **2** presumably corresponds to further decomposition.

Cyclic voltammetry for compounds **1** and **2**

The cyclic voltammograms of compounds **1** and **2** were recorded in acetonitrile and are shown in Fig. 1 (see ‘Experimental’ for details of measurement). Comparing the two voltammograms it can be seen that both compounds undergo an irreversible oxidation with compound **2** ($X=H$) being more easily oxidized than compound **1** ($X=F$). Thus, compound **1** shows no discernible oxidation until a potential of about 1.4 V (versus SCE) is reached whereas oxidation of compound **2** starts at about 0.8 V. The oxidized acyl species are relatively short-lived and decompose or rearrange to non-acyl products; this is supported by IR studies which show the decrease of the acyl $\nu(\text{CO})$ bands whereas the $\nu(\text{CO})$ bands of the terminal carbonyls are relatively unchanged. The reduction of these oxidation products is similar to that previously reported for the compounds $\text{CpFe(CO)}_2\text{COMe}$ [9, 10].

Thus the main conclusion from this electrochemical study is that the fluorinated compound is more stable to oxidation by about 600 mV than its hydrocarbon

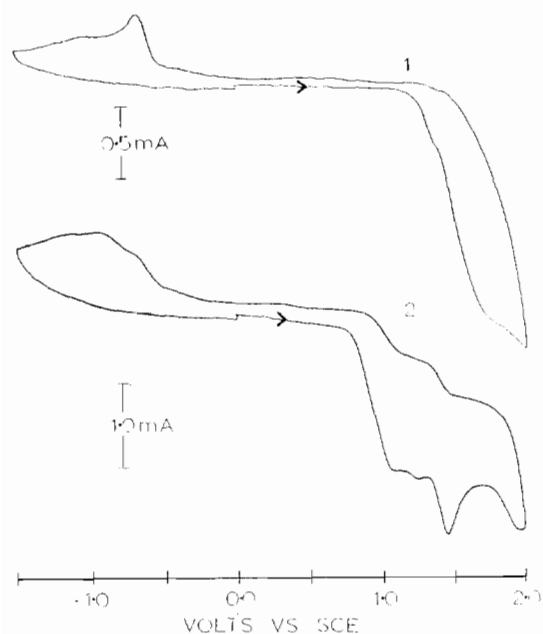


Fig. 1. Cyclic voltammograms of compounds **1** and **2** (see 'Experimental' for conditions of measurement).

analogue. This finding is supported by reactivity and structural studies.

Reactivity of compounds **1** and **2**

Compound **1** shows no reaction with HPF_6 , AgPF_6 or I_2 under the conditions used, whereas compound **2** shows reaction with all these reagents under the same conditions. For the reaction of **2** with I_2 , $\nu(\text{CO})$ bands are observed which correspond to $\text{CpFe}(\text{CO})_2\text{I}$, suggesting that the $\text{Fe}-\text{C}(\text{acyl})$ bond is cleaved by iodine. The fact that **1** does not react with iodine suggests a very strong iron-acyl bond in **1**; crystallographic evidence (see later) further supports this. After 27 h of refluxing in THF with PPh_3 , **1** showed (by IR) about 12% substitution by PPh_3 , whereas **2** showed only about 2% substitution. This is in agreement with the $\text{Fe}-\text{C}(\text{terminal carbonyl})$ bond being stronger in **2** than in **1** which is consistent with IR data. Thus the fluorocarbon compound **1** has a stronger $\text{Fe}-\text{C}(\text{acyl})$ bond than **2** but is more susceptible to substitution of CO by PPh_3 . The unreactivity of **1** towards protonation by HPF_6 may be indicative of electron withdrawal by the fluorocarbon moiety from the acyl groups.

Crystal structure of **1**

As far as we know, this is the first structural study on a fluorocarbon-bridged diacyl compound. The molecular structure of **1** is shown in Fig. 2. Bond lengths and bond angles are given in Table 2. The molecule has no symmetry although the general shape is very

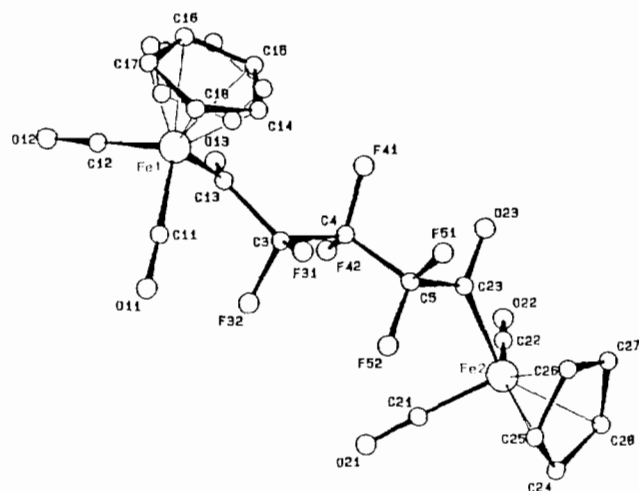


Fig. 2. Molecular structure of $\text{FpC}(\text{O})(\text{CF}_2)_3\text{C}(\text{O})\text{Fp}$. Cp disorder only shown for one ring.

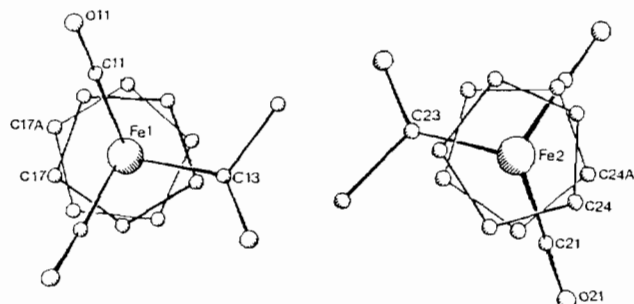


Fig. 3. Projection of the two $\text{FpC}(\text{O})\text{C}$ fragments in **1** onto their respective Cp planes.

similar to that of $[\text{CpRu}(\text{CO})_2]_2[\mu-(\text{CH}_2)_5]$ [11]. In both molecules, the Cp rings are on the same side of the molecule; the dihedral angle between the normals to the Cp planes is $76.4(5)^\circ$ in **1**, and $79.5(4)^\circ$ in the Ru complex. This relative *cis* orientation is presumably allowed by the length of the bridging chain. In similar compounds with shorter chains, the relevant dihedral angles are much greater [12].

As shown in Table 3, the bond lengths $\text{Fe}-\text{C}(\text{Cp})$ and $\text{C}-\text{O}(\text{acyl})$ in **1** agree well with those in similar molecules such as $\text{Fp}(\text{CH}_2)_n\text{Fp}$ ($n=3, 4$) [12], $\text{Fp}-\text{CH}_2\text{CO}_2\text{H}$ [13], $\text{FpC}(\text{Me})\text{CH}_2\text{C}(\text{CN})_2\text{C}(\text{CN})_2\text{CH}_2$ [14] and $\text{CpFe}(\text{CO})(\text{PPh}_3)\text{C}(\text{O})\text{R}$ [15–18]. It is interesting to note however, that the $\text{Fe}-\text{C}(\text{acyl})$ bonds in **1** are significantly shorter than those in three compounds of the type $\text{CpFe}(\text{CO})(\text{PPh}_3)\text{C}(\text{O})\text{R}$. Shortening of this bond in the fluorocarbon complex may be expected since it is found that metal-carbon bond lengths in σ -perfluoroalkyl complexes are usually shorter than those in corresponding hydrocarbon complexes [19]. The presence of PPh_3 in the latter complexes is not expected to have much effect on the length of the $\text{Fe}-\text{C}(\text{acyl})$ bond. It has been observed that the $\text{Fe}-\text{C}(\text{acyl})$ bond

TABLE 2. Bond lengths (Å) and angles (°) with (e.s.d.s) for FpC(O)(CF₂)₃C(O)Fp

Fe1–C11	1.782(8)	Fe2–C21	1.762(8)	C13–C3	1.556(11)
Fe1–C12	1.753(8)	Fe2–C22	1.735(9)	C3–C4	1.530(10)
Fe1–C13	1.953(8)	Fe2–C23	1.929(9)	C4–C5	1.541(12)
Fe1–C14	2.10(2)	Fe2–C24	2.09(1)	C5–C23	1.543(12)
Fe1–C15	2.14(2)	Fe2–C25	2.09(1)	C11–O11	1.124(9)
Fe1–C16	2.10(1)	Fe2–C26	2.10(1)	C12–O12	1.142(10)
Fe1–C17	2.12(2)	Fe2–C27	2.09(1)	C21–O21	1.130(10)
Fe1–C18	2.13(2)	Fe2–C28	2.09(1)	C22–O22	1.157(11)
Fe1–Cp1 ^a	1.93(4)	Fe2–Cp2 ^a	1.90(2)	C3–F31	1.305(10)
Fe1–C14A	2.08(2)	Fe2–C24A	2.15(3)	C3–F32	1.376(9)
Fe1–C15A	2.09(2)	Fe2–C25A	2.14(3)	C4–F41	1.335(8)
Fe1–C16A	2.10(3)	Fe2–C26A	2.13(3)	C4–F42	1.328(9)
Fe1–C17A	2.09(3)	Fe2–C27A	2.14(3)	C5–F51	1.369(11)
Fe1–C18A	2.08(3)	Fe2–C28A	2.15(3)	C5–F52	1.343(9)
C13–O13	2.213(10)	C23–O23	1.185(10)		
C11–Fe1–C12	95.2(4)	C21–Fe2–C22	92.8(4)		
C11–Fe1–C13	93.8(4)	C21–Fe2–C23	95.5(4)		
C12–Fe1–C13	86.9(4)	C22–Fe2–C23	88.0(4)		
Fe1–C11–O11	177.1(7)	Fe2–C21–O21	177.5(8)		
Fe1–C12–O12	178.0(8)	Fe2–C22–O22	178.1(8)		
Fe1–C13–O13	127.9(6)	Fe2–C23–O23	127.4(7)		
Fe1–C13–C3	119.4(6)	Fe2–C23–C5	122.0(6)		
O13–C13–C3	112.7(7)	O23–C23–O5	109.6(7)		
C13–C3–F31	114.2(7)	C23–C5–F51	110.3(7)		
C13–C3–F32	107.4(6)	C23–C5–F52	112.9(7)		
F31–C3–F32	103.6(7)	F51–C5–F52	104.2(7)		
C4–C3–F31	108.6(7)	C4–C5–F51	106.1(7)		
C4–C3–F32	105.9(6)	C4–C5–F52	108.8(6)		
C13–C3–C4	116.2(6)	C23–C5–C4	113.8(7)		
C3–C4–F41	105.2(6)	C5–C4–C3	118.4(6)		
C3–C4–F42	108.9(6)	C5–C4–F41	109.5(6)		
F41–C4–F42	109.5(6)	C5–C4–F42	105.3(6)		

^aCp1 and Cp2 are respective centroids of the Cp rings.

TABLE 3. Bond length comparisons (Å) in related compounds

Compound	Fe–C (carbonyl)	Fe–C (acyl)	Fe–C (alkyl)	Fe–C ^a (Cp)	C–O (carbonyl)	C–O (acyl)	Reference
Fp(CH ₂) _n Fp (<i>n</i> = 3, 4)	1.74(1) ^a		2.08(1)	2.11(1)	1.15(1) ^a		12
FpCH ₂ CO ₂ H	1.72(2) ^a		2.06(2)	2.15(2)	1.17(3)		13
FpC(Me)CH ₂ C(CN) ₂ C(CN) ₂ CH ₂	1.754(2) ^a		2.096(2)	2.107(3)	1.148(2) ^a		14
CpFe(CO)(PPh ₃){COCH(Me)Et}	1.733(3)	1.964(3)		2.121(3)	1.148(4)	1.207(4)	15
CpFe(CO)(PPh ₃)COCH ₃	1.700(14)	1.964(12)		2.136(5)	1.193(17)	1.228(13)	16
CpFe(CO)(PPh ₃)R ^b	1.705(9)	1.964(10)		2.109(9)	1.174(11)	1.216(11)	17
FpC(O)(CF ₂) ₃ C(O)Fp	1.758(8) ^a	1.941(6) ^a		2.11(2)	1.41(1) ^a	1.20(1) ^a	this work

^aMean. ^bR = COCH₂CHCHCOOCHCH(Me)CH=CH.

lengths in η^1 -hydrocarbon complexes of iron ‘depends markedly on the character of the α -carbon atom of the organic ligand but is much less strongly influenced by the nature of the other ligands on the metal’ [20].

C–Fe–C bond angles show that the Fe coordination sphere fits the currently accepted pseudo-octahedral description for similar compounds with Cp occupying three octahedral sites [21]. As observed in Fp(CH₂)_nFp

[12], the OC–Fe–CO angle in **1** is greater than 90°, due to repulsion between the carbonyl groups.

Figure 3 shows the projections of the two CpFe(CO)₂C(O) fragments onto the planes containing the Cp rings. In each case, the orientation of the major Cp ring contribution is almost identical to that found in Fp(CH₂)_nFp [12]; the carbonyl groups lie *between* ring carbon atoms in projection. The minor Cp ring

on Fe1 has a similar orientation, but the minor ring on Fe2 has one carbon atom which eclipses a carbonyl carbon atom. In agreement, this Cp ring orientation is only 20% populated; the minor orientation on Fe1 is 35% populated.

Conclusions

Evidence for the strengthening of the Fe–C(acyl) bond in the fluorocarbon complex relative to its hydrocarbon analogue, is given by IR data, reactivity studies, cyclic voltammetry and structural data. It appears, therefore, that processes responsible for the relative shortening of Fe–C(alkyl) bonds and subsequent increased resistance to oxidation in α -perfluoroalkyl complexes, persist even when the metal atom and the fluorocarbon chain are separated by an acyl group. Furthermore, the Fe–C(carbonyl) bonds in the present fluorocarbon complex are relatively longer than those in the hydrocarbon complex, as shown by IR and structural data.

Supplementary material

Tables of observed and calculated structure factors, fractional atomic coordinates, anisotropic temperature factors and non-bonded atomic contacts as well as a crystal packing diagram for compound **1** are available from the authors on request.

Acknowledgements

We thank the University of Cape Town, Peninsula Technikon and the FRD for support and Dr M. L. Niven for collecting the X-ray data.

References

- 1 J. P. Collman, L. S. Hegedus, J. R. Norton and R. G. Finke, *Principles and Applications of Organotransition Metal Chemistry*, University Science Books, Mill Valley, CA, 1987, p. 65.
- 2 R. B. King and M. B. Bisnette, *J. Organomet. Chem.*, **2** (1964) 15.
- 3 R. B. King, *J. Am. Chem. Soc.*, **85** (1963) 1918.
- 4 A. C. T. North, D. C. Phillips and F. S. Mathews, *Acta Crystallogr., Sect. A*, **24** (1968) 351.
- 5 G. M. Sheldrick, in H. Schenk, R. Olthof-Hazenkamp, H. van Koningsveld and G. C. Bassi (eds.), *Computing in Crystallography*, Delft University Press, Delft, 1978, pp. 34–42.
- 6 D. T. Cromer and J. B. Mann, *Acta Crystallogr., Sect. A*, **24** (1968) 321.
- 7 D. T. Cromer and D. Liberman, *J. Chem. Phys.*, **53** (1970) 1891.
- 8 W. D. S. Motherwell, *PLUTO*, program for plotting molecular and crystal structures, Cambridge University, UK, 1974.
- 9 R. H. Magnuson, S. Zulu, W. Tsai and W. P. Giering, *J. Am. Chem. Soc.*, **102** (1980) 6888.
- 10 R. J. Klinger and J. K. Kochi, *J. Organomet. Chem.*, **202** (1980) 49.
- 11 K. P. Finch, J. R. Moss and M. L. Niven, *Inorg. Chim. Acta*, **166** (1989) 181.
- 12 L. Pope, P. Sommerville, M. Laing, K. Hindson and J. R. Moss, *J. Organomet. Chem.*, **112** (1976) 309.
- 13 J. K. P. Ariyaratne, A. M. Bierrum, M. L. H. Green, M. Ishaq, C. K. Prout and M. G. Swanwick, *J. Chem. Soc. A*, (1969) 1309.
- 14 M. R. Churchill and S. W.-Y. Ni Chang, *J. Am. Chem. Soc.*, **95** (1973) 5931.
- 15 G. J. Baird, J. A. Bandy, S. G. Davies and K. Prout, *J. Chem. Soc., Chem. Commun.*, (1983) 1202.
- 16 T. G. Attig, R. G. Teller, S.-M. Wu, R. Bau and A. J. Wojcicki, *J. Am. Chem. Soc.*, **101** (1979) 619.
- 17 G.-H. Lee, S.-M. Peng, S.-F. Lush and R.-S. Lin, *J. Organomet. Chem.*, **349** (1988) 219.
- 18 S. G. Davies, I. M. Dordor-Hedgecock, K. H. Sutton, J. C. Walker, C. Bourne, R. T. Jones and K. Prout, *J. Chem. Soc. Chem. Commun.*, (1986) 607.
- 19 R. D. W. Kemmitt and D. R. Russell, in G. Wilkinson (ed.), *Comprehensive Organometallic Chemistry*, Vol. 5, Pergamon, Oxford, 1982, p. 65.
- 20 M. D. Johnson, in G. Wilkinson (ed.), *Comprehensive Organometallic Chemistry*, Vol. 4, Pergamon, Oxford, 1982, p. 343.
- 21 J. I. Seeman and S. G. Davies, *J. Am. Chem. Soc.*, **107** (1985) 6522.